ISSN 1346-7565

Acta Phytotax. Geobot. 77 (1): 1–21 (2026)
doi: 10.18942/apg.202519

Phylogeography of the Temperate Grassland Species *Pulsatilla cernua* (Ranunculaceae): Insights into the Timing of Migration and Range Shifts in Japan

Hiroaki Saito[1], Noriyuki Fujii[2], Hajime Ikeda[3], Takaya Iwasaki[4], Nana Goto[1], Yoshihisa Suyama[5], Ayumi Matsuo[5], Andrey E. Kozhevnikov[6], Zoya V. Kozhevnikova[6], Jae-Hong Pak[7], Kyung Choi[8], Tiangang Gao[9] and Akiko Soejima[2,*]

[1]Department of Science, Graduate School of Science and Technology, Kumamoto University, 2-39-1 Kurokami, Chuo-ku, Kumamoto 860-8555, Japan; [2]Division of Natural Science, Faculty of Advanced Science and Technology, Kumamoto University, 2-39-1 Kurokami, Chuo-ku, Kumamoto 860-8555, Japan, [*]soejima@kumamoto-u.ac.jp (author for correspondence); [3]Graduate School of Arts and Sciences, The University of Tokyo, 3-8-1 Komaba, Meguro-ku, Tokyo 153-8902, Japan; [4]Natural Science Division, Faculty of Core Research, Ochanomizu University, 2-1-1 Otsuka, Bunkyo-ku, Tokyo 112-8610, Japan; [5]Kawatabi Field Science Center, Graduate School of Agricultural Science, Tohoku University, 232-3 Yomogida, Naruko-onsen, Osaki, Miyagi 989-6711, Japan; [6]Federal Scientific Center of the East Asia Terrestrial Biodiversity, Far Eastern Branch of the Russian Academy of Sciences, Vladivostok, Russia; [7]Research Institute for Dok-do and Ulleung-do Island, Department of Biology, School of Life Sciences, Kyungpook National University, 80 Daehak-ro, Buk-gu, Daegu, 41566, Republic of Korea; [8]Division of Forest Biodiversity, Korea National Arboretum, 415 Gwangneungsumokwon-ro, Soheul-eup, Pocheon-si, Gyeonggi-do, 11186, Republic of Korea; [9]State Key Laboratory of Systematic and Evolutionary Botany, Institute of Botany, Chinese Academy of Sciences, Beijing 100093, China

A group of temperate grassland plant species, referred to as the 'Mansen elements,' is found in Japan and extensively distributed in the grasslands of continental East Asia. It has been considered that these species are remnants of once-expanded grasslands in Japan during a colder geological era. However, the detailed phylogeographic history, including migration age and distributional changes within Japan for these species, remains unresolved. To elucidate the phylogeographic history of the Mansen elements, we investigated the genetic structure and phylogeny of the populations of *Pulsatilla cernua*, one of the Mansen elements, using single-nucleotide polymorphisms (SNPs) obtained from multiplexed inter-simple sequence repeat genotyping by sequencing (MIG-seq). The phylogenetic analysis indicates a continental origin and migration route via the Korean Peninsula for *P. cernua*. The DIYABC and the genetic structure analyses suggest that the divergence between the continental and Japanese populations occurred in the late stage of the Last Glacial Period (LGP). Although the estimated divergence time is not fully constrained, it is suggested that an initial expansion in Japan occurred before the Last Glacial Maximum (LGM). This once-expanded distribution area was subsequently fragmented during the coldest climate, followed by a secondary expansion after the LGP. This represents the first documented instance among the Mansen element species in which secondary range expansion brought fragmented populations into secondary contact.

Keywords: continental East Asia, genetic structure, Japanese Archipelago, Mansen elements, migration, MIG-seq, phylogeography, temperate grassland

The Japanese Archipelago is located on the eastern coast of continental East Asia in the middle latitudes and is included in the Asian monsoon zone which brings more than 1,000 mm of

rainfall per year (Mushiake 2001). Because of the warm and humid climate, the vegetation of Japan is predominantly composed of forests covering 67 percent of the total land area (Ministry of the Environment of Japan 2016, Ushimaru *et al.* 2018). Under such an environment, natural grasslands exist in very limited areas, such as in alpine zones, riparian areas, and coasts (Ushimaru *et al.* 2018). It is considered, however, that grassland vegetation occupied a more extensive area in Japan during the colder and drier climate of the Last Glacial Period (LGP) (Okamura *et al.* 1998, Noshiro 2017). After the LGP, a warming climate led to forest expansion, consequently resulting in a decline in area of natural grasslands and an increase in the human population (Ushimaru *et al.* 2018). That era also witnessed the rise of semi-natural grasslands that emerged from human activities such as fire use (Ushimaru *et al.* 2018). Those semi-natural grasslands are considered to have been the most widely distributed grassland type during the prehistoric age of Japan (Kawano *et al.* 2012, Miyabuchi *et al.* 2012, Ushimaru *et al.* 2018). In response to the decline in natural grassland areas due to the warming climate, grassland species may have taken refuge in semi-natural grasslands (Yamaura *et al.* 2019).

Among such grassland species, there are temperate grassland species known as Mansen elements, primarily distributed in the western Japan (Koidzumi 1931, Hotta 1957, Kitamura 1957, Murata 1977, 1988). They are also distributed in the Korean Peninsula and northeastern China, or have close relatives in those regions. In Japan, their distribution is largely restricted to the area between northern Kyushu and central Honshu. Although some Mansen elements extend from Kyushu to northeastern Honshu, they are absent from Hokkaido, despite the latitude of Hokkaido being comparable to or even lower than that of northeastern China. Based on the distribution pattern of the Mansen elements, previous researchers considered that they originated on the continental East Asia and migrated to the Japanese Archipelago via the Korean Peninsula during a relatively recent cold age (Koidzumi 1931, Hotta 1957, Kitamura 1957, Murata 1977, 1988).

Recently, several phylogeographic studies have attempted to examine the origin and migration routes of the Mansen elements (Sata *et al.* 2021, Sakaba *et al.* 2023, Fujii *et al.* 2025). Those studies suggested that the Mansen elements originated in continental East Asia and migrated to Japan during the LGP. Although the Korean Peninsula route was not consistently designated, it was inferred in the case of *Viola orientalis* (Maxim.) W. Becker. Their subsequent range shifts within Japan, however, appear to have varied among species. For instance, Sata *et al.* (2021) indicated that *V. orientalis* migrated to Japan during the LGP and that populations were subsequently separated into the Kyushu and Honshu regions after the Last Glacier Maximum (LGM). Similarly, analyses by Fujii *et al.* (2025) demonstrated that populations of *Potentilla discolor* Bunge also experienced a separation between Kyushu and Honshu, as observed in *V. orientalis*. In another example, Sakaba *et al.* (2023) indicated that *Tephroseris kirilowii* (Turcz. ex DC.) Holub migrated to Japan around the beginning of the LGM, but expanded toward northeastern Japan once after the LGM. Adding to these findings, Kurata *et al.* (2024) investigated *Geranium krameri* Franch. et Sav., one of the Mansen elements, and suggested that the weak genetic differentiation observed in this species may reflect a historically continuous distribution and substantial gene flow during the Ice Age. These results collectively suggest that the Mansen elements migrated to Japan under a colder climate than today. However, it remains unclear whether they subsequently experienced repeated episodes of isolation, fragmentation, and range expansion within Japan.

Given the species specific patterns of range shift observed in the Mansen elements, we suspect that *Pulsatilla cernua* (Thunb.) Bercht. et J. Presl., another Mansen element, may exhibit a unique demographic history within Japan. Despite its fragmented distribution across the Japanese Archipelago, *P. cernua* has the widest range among the Mansen elements in Japan, extending from southern Kyushu to northeastern Honshu, suggesting the involvement of complex historical processes such as repeated cycles of range expan-

sion and contraction, or localized persistence. Previous studies (Takaishi *et al.* 2019) have indicated genetic homogeneity among Japanese populations based on chloroplast DNA haplotypes, but the resolution of such data is insufficient to distinguish between scenarios involving a single post-LGM expansion and multiple episodes of range expansion and contraction. Moreover, the divergence time between the continental and Japanese populations remains unclear. To address these questions, we employed high-resolution single-nucleotide polymorphism (SNP) data obtained from multiplexed inter-simple sequence repeat genotyping by sequencing (MIG-seq) analysis to uncover the genetic structure of populations of *Pulsatilla cernua* across Japan. Additionally, DIYABC analysis was conducted to infer the history of range expansion of *P. cernua*, including divergence times. By integrating these approaches, we aimed to estimate the route and timing of migration and test whether *P. cernua* experienced a single expansion or underwent multiple cycles of expansion and contraction. In addition, our study compared distribution patterns and genetic structure among other Mansen elements, thereby providing a deeper understanding of the historical processes within the Japanese Archipelago.

Materials and Methods

Plant materials and DNA extraction

We collected 398 individuals of *Pulsatilla cernua* from 32 populations in Japan, Korea, Russia, and China (Table 1, Fig. 1). Additionally, two

TABLE 1. Voucher information.

Taxon	Population	Locality	Voucher	No. of samples used in MIG-seq analysis	Geological group
Pulsatilla cernua	J1	Kuzumaki, Iwate	*Takaishi 160608*	14	East-1, Japan
	J2	Hachimantai, Iwate	*Soejima & Takaishi 131008*	15	East-1, Japan
	J3	Shirataka, Yamagata	*Soejima & Takaishi 140614*	16	East-1, Japan
	J4	Inzai, Chiba	*Nishiihiro 130930*	10	East-1, Japan
	J5	Aizuwakamatsu, Fukushima	*Nemoto 190607*	16	East-1, Japan
	J6	Shioya, Tochigi	*Takaishi 130421*	16	East-1, Japan
	J7	Hokuto, Yamanashi	*Soejima & Takaishi 140806*	5	East-2, Japan
	J8	Ueda, Nagano	*Soejima & Takaishi 140807-3*	14	East-2, Japan
	J9	Ueda, Nagano	*Soejima & Takaishi 140807-2*	10	East-2, Japan
	J10	Nanto, Toyama	*Mototani 200412*	9	East-2, Japan
	J11	Mino, Gifu	*Takahashi 28027*	11	East-2, Japan
	J12	Kobe, Hyogo	*Nakahama 191020-1*	10	West-1, Japan
	J13	Yabu, Hyogo	*Nakahama 191020-2*	16	West-1, Japan
	J14	Wajiki, Tokushima	*Soejima 131101*	16	West-1, Japan
	J15	Wake, Okayama	*Soejima & Takaishi 150617*	11	West-2, Japan
	J16	Shimanto, Kochi	*Soejima 130730*	4	West-1, Japan
	J17	Sanbe, Shimane	*Soejima & Takaishi 150618-2*	12	West-1, Japan
	J18	Sanbe, Shimane	*Soejima & Takaishi 150618-1*	12	West-1, Japan
	J19	Kushima, Miyazaki	*Soejima 130808*	16	West-2, Japan
	J20	Mine, Yamaguchi	*Oota & Sakaba S19-030*	16	West-2, Japan
	J21	Namino, Kumamoto	*Soejima & Takaishi 130520*	12	West-2, Japan
	J22	Asagiri, Kumamoto	*Soejima et al. S20-007*	16	West-2, Japan
	J23	Kiyama, Saga	*Takaishi 150404*	9	West-2, Japan
	K1	Gangneung, Gangwon	*Soejima et al. S-172*	16	South Korea
	K2	Yeongcheon, Gyeongsangbuk	*Soejima et al. S-127*	16	South Korea
	K3	Jeju, Jeju	*Soejima & Takaishi 160616*	16	South Korea
	R1	Vodopadnoye, Primorsky	*Soejima & Fujii S-008*	11	Russia
	R2	Turilog, Primorsky	*Soejima et al. 150506*	12	Russia
	R3	Kommissarovo, Primorsky	*Soejima et al. S-005*	12	Russia
	R4	Pokrovka, Primorsky	*Soejima & Fujii S-038*	2	Russia
	R5	Primorsk, Primorsky	*Soejima et al. S-027*	16	Russia
	C1	Jilin, Jilin	*Soejima & Fujii S-053*	11	China
P. chinensis		Primorsk, Primorsky, Russia	*Soejima et al. 044*	2	
P. dahurica		Primorsk, Primorsky, Russia	*Soejima et al. 034*	3	

FIG. 1. Geographic distribution of the sampled populations of *Pulsatilla cernua*. Lines indicate borders between genetically differentiated population groups in the phylogenetic tree (Fig. 2). The names of the population groups are in italics.

individuals from one population of *Pulsatilla chinensis* (Bunge) Regel and three individuals from one population of *P. dahurica* (Fisch. ex DC.) Spreng., which are considered closely related to *P. cernua* (Sramkó *et al.* 2019), were also collected to be used as outgroups (Table 1). The vouchers are deposited in Kumamoto University. These three species are known to have 16 somatic chromosomes and considered to be diploid (Lee 1967, Yurtsev & Zhukova 1982, Zhang 2006, Sramkó *et al.* 2019). The leaves were dried in silica gel and whole genomic DNA was extracted using a modified cetyl-trimethyl-ammonium-bromide (CTAB) method (Doyle & Doyle 1987).

MIG-seq analysis

Genome-wide SNP data were obtained using the MIG-seq method (Suyama & Matsuki 2015). A MIG-seq library was constructed using 403 individuals of the three species. Sequencing was performed using the Illumina MiSeq platform with a MiSeq Reagent v.3 150 cycle kit (Illumina, San Diego, CA, USA). Fragments were read in both directions using paired-end sequencing. After removing primer regions, sequences shorter than 71 bp and low-quality reads with an average quality value of 4 bases, using the default setting of the sliding window, greater than 15 were filtered in the single-end mode of Trimmomatic (Bolger *et al.* 2014), and SNP detection was performed on the Illumina reads treated as single-end using Stacks v.2.55 (Catchen *et al.* 2011) with the following parameter settings: maximum distance (in nucleotides) allowed between stacks (M = 2), minimum depth of coverage required to create a stack (m = 5), maximum distance allowed to align secondary reads to primary stacks (N = 4), and the number of mismatches allowed between sample loci when building the catalog (n = 2). These nucleotide sequence data were deposited in

the DDBJ database with the accession number of PRJDB18174 (DRR570255-DRR570657).

Phylogenetic Relationships Based on MIG-seq SNP Data

A maximum likelihood phylogenetic tree was constructed using the MIG-seq SNP dataset prepared above. *Pulsatilla chinensis* and *P. dahurica* were used as outgroups. We then used the 'populations' command to set the upper limit of heterozygosity to 0.6 (max-obs-het = 0.6), the minimum number of minor alleles to 3 (min-mac = 3), and the SNPs shared by more than 10% of all samples (R = 0.1). A Python script (github.com/btmartin721/raxml_ascbias) was run in raxml_ascbias.py to remove potential invariant sites. After removing invariant sites, we constructed a maximum likelihood phylogenetic tree of *P. cernua* using RAxML v.8.2.10 (Stamatakis 2014) with Lewis confirmation bias correction: -m GTRGAMMA --asc-corr = lewis (Leaché *et al.* 2015) and 1000 bootstrap replicates.

Genetic structure based on MIG-seq SNP data

To estimate the genetic structure of *P. cernua*, a Bayesian clustering analysis based on SNP data was performed using STRUCTURE v.2.3.4 (Pritchard *et al.* 2000). Only the samples of *P. cernua* were included in this analysis. Stacks v.2.5.5 (Catchen *et al.* 2011) was used for filtering as follows: 'ustacks' command was used to set the minimum number of identical reads required to create a stack to 5 (m = 5), 'populations' commands R = 0.5 was used to retrieve SNPs shared by more than 50% of all the samples and max-obs-het = 0.6 to remove SNPs with high heterozygosity (>0.6). Furthermore, one SNP was randomly taken from each locus using the 'write-random-snp' option. Using TASSEL5 (Bradbury *et al.* 2007), missing data more than 50% and SNPs with minor allele frequencies (MAF) less than 0.01 were removed. STRUCTURE parameters were 'admixture model' for the ancestry model, 'allele frequencies correlated' for the allele frequency model, and '1-10 clusters (*K*)' for the number of virtual ancestral populations. For each 1-10 clusters (*K*), 100,000 burn-in followed by 100,000 MCMC steps were performed with 10 independent runs. Data ΔK (Evanno *et al.* 2005) and Ln probabilities of the data, LnP (*K*), were calculated using STRUCTURE Harvester v.2.3.4 (Earl & von Holdt 2012). To create bar plots, we used the online CLUMPAK (Kopelman *et al.* 2015). Genetic distances between individuals were calculated using TASSEL5 and a phylogenetic network was constructed using the NeighborNet method (Bryant & Moulton 2004) with SplitsTree v.4.14 (Huson & Bryant 2006).

Population genetic indices

The values of genetic diversity for each population, including the mean number of alleles per locus (*N*a), the number of valid alleles per locus (*N*e), the Shannon Information Index (*I*), the observed value of heterozygosity (H_O) (Nei, 1987), the expected value of heterozygosity (H_E), the expected value of unbiased heterozygosity (uH_E) and the coefficient of inbreeding (F_{IS}) were estimated using GenAlEx v.6.51b2 (Peakall & Smouse 2012). We also calculated the number of alleles (Num), the number of effective alleles (Eff_num), the heterozygosity (H_S) in the population (Nei 1987), and inbreeding coefficient (G_{IS}) using GenoDive v.3.04 (Meirmans & Tienderen 2004). The genetic diversity and differentiation statistics for each cluster detected in the results of STRUCTURE analyses were calculated for the expected value of heterozygosity (H_O), the heterozygosity within a subpopulation (H_S), the inbreeding coefficient (G_{IS}), the fixation index (G_{ST}) (Nei 1987), the standard fixed index (G'_{ST}) (Nei 1987, Hedrick 2005), the modified standardized fixed index (G''_{ST}) (Meirmans & Hedrick 2011), and the population differentiation index (*Dest*) (Jost 2008) were also calculated.

Estimating population dynamics using approximate Bayesian computation (ABC) analysis

We estimated population demographic history of *P. cernua* by the ABC method using DIYABC v.2.1 (Cornuet *et al.* 2014). Considering the genetic structure in STRUCTURE, NeighborNet analysis, and the clades in phylogenetic analysis, we performed the analyses in three

steps.

To infer whether populations from western Japan or eastern Japan originated from the other, the 32 populations were divided into the following three groups according to $K = 3$ of the STRUCTURE analysis: the populations of eastern Japan (J1–J11), the populations of western Japan (J12–23), and the continental populations (C1, K1–2, R1–5) in the DIYABC-1 analysis. After multiple preliminary analyses using various population statistics, three scenarios were developed to estimate population dynamics. The scenarios were characterized by several demographic parameters, including divergence times in generation (t1, t2) and effective population size (N1, N2, N3, Nt). For each population and each population pair, we used 10 summary statistics from genetic diversity, genetic distance by F_{ST}, and genetic distance by Nei's. A training set included 100,000 datasets was simulated for each scenario. Each scenario was pre-evaluated by Principal Component Analysis (PCA) within DIYABC. To select the best scenario, the approximate likelihood of each scenario was calculated by logistic regression in DIYABC. The effective population size and the posterior distribution of the divergence times for the scenario with the best approximate likelihood for each scenario was estimated as a ratio to the mean effective population size MeanN.

To infer whether the West-1 or the West-2 originated from the other, the 29 populations, excluding populations with mixed structure (J10, J11, J15), were classified into the following four groups according to $K = 4$ of the STRUCTURE analysis: populations of East Japan (J1–9), populations of West-1 (J12–14, J17–18) , the populations of West-2 (J16, J19–23), and the continental populations (C1, K1–2, R1–5) in the DIYABC analysis. After multiple preliminary analyses using various population statistics, three scenarios were created to estimate population dynamics. These scenarios were characterized by several demographic parameters, including divergence times in generation (t1, t2, t3) and effective population size (N1, N2, N3, N4, Nt2). For each population and each population pair, eight summary statistics were used from genetic diversity, genetic distance by F_{ST}, and genetic distance by Nei's. A training set included 100,000 datasets was simulated for each scenario.

To infer which hybridization happened earlier between West-1 and West-2 or between West-1 and East Japan, the 29 populations were grouped into six: populations of East Japan (J1–9), populations of Toyama (J10) and Gifu (J11), populations of West-1 (J12–14, J17, J18), population of Okayama (J15), populations of West-2 (J16, J19–J23), and continental populations (C1, K1–2, R1–5) in the DIYABC-3 analysis. After multiple preliminary analyses using various population statistics, four scenarios were created to estimate population dynamics. The scenarios examined how the six large group populations diverged. They were characterized by several demographic parameters, including divergence times in generation (t1–t5) and effective population size (N1–N6). The admixture rates 'r1' and '1-r1' and 'r2' and '1-r2' in each scenario represent the genetic contribution of the ancestral population and indicate the likelihood of admixture events. For each population and each population pair, we used eight summary statistics from genetic diversity, genetic distance by F_{ST}, and genetic distance by Nei's. A training set included 100,000 datasets was simulated for each scenario.

Ecological niche modeling analysis

The potential distribution of *Pulsatilla cernua* during the present, the middle Holocene (MID), about 6,000 years ago (ya), the LGM, about 22,000 ya, and the Last Interglacial Period (LIG), about 120,000~140,000 ya, was reconstructed using Maxent v.3.4.1 (Phillips *et al.* 2017). A total of 374 occurrence points were obtained from the databases of Kagoshima University Museum (KAG), Science Museum Net (S-net), Global Biodiversity Information Facility (GBIF), Chinese Virtual Herbarium (CVH), accessed during August–September 2022, and the authors' field observations from 2013 to 2021. To reduce the difference in the number of occurrence points between Japan and the continent, the spatial filtering method was used to adjust the density of locations by creating a grid of a certain size and treat-

ing multiple locations within a grid as a single location, or by thinning out locations within a certain distance (Boria *et al*. 2014, Fourcade *et al*. 2014, Varela *et al*. 2014). Therefore, a grid of 1.0° units was created, and the total distribution information used to analyze was 65 points.

Nineteen bioclimatic variables with a spatial resolution of 2.5 arc-min squares (ca. 5 × 5 km) were extracted from WorldClim1.4 (Hijmans *et al*. 2005, http://www.worldclim.org), and seven variables with low Pearson's correlation coefficient ($r < 0.8$) were selected to construct the present distribution model (Table 2). The analyzed area was adapted to the area roughly covering all 65 occurrence points in a square of latitude and longitude. Two paleoclimate models, the community climate system model (CCSM4) (Gent *et al*. 2011) and the earth system model based on the model for interdisciplinary research on climate (MIROC-ESM) (Watanabe *et al*. 2011) were used to predict the distributions in the MID and LGM. To predict LIG, we used a spatial resolution of 30 arc-sec (about 1 × 1 km) (Otto-Bliesner *et al*. 2006). Each model was run with 10 replicates using a cross-validation approach and the results were averaged. Other settings followed the default parameters of Maxent.

The area under the receiver operating characteristic curve (AUC) was used to assess overall model performance. Additionally, a confusion matrix was calculated using R v.4.3.3. For this calculation, a dataset consisting of 65 presence points, which were prepared above and used in the MaxEnt modeling, and 9,999 pseudo-absence points, which were generated within the MaxEnt modeling process, was used. To prioritize sensitivity and minimize false negatives, the 10% logistic threshold—a standard metric in ecological niche modeling—was applied. This threshold was used to evaluate the present climate model, and one representative result from multiple iterations was selected to reflect the general performance of the model. Based on the confusion matrix, evaluation metrics, including accuracy, sensitivity, precision, F1-score, and omission/commission errors, were calculated. These metrics provide a detailed assessment of the model's predictive performance and were derived following the guidelines of Pearce & Ferrier (2000) and Powers (2011).

To assess the influence of each environmental variable on the model's predictions, percent contribution and permutation importance were calculated. Percent contribution estimates the relative influence of each variable during the training process, based on its effect on model optimization. Permutation importance evaluates the decrease in model performance when the values of a given variable are randomly permuted while keeping other variables unchanged. Both metrics were normalized and expressed as percentages, and the final values were averaged over 10 replicate runs to ensure robustness and representativeness of the results.

Results

Phylogenetic analysis

Figure 2 shows a phylogenetic tree of *Pulsatilla cernua* and two outgroup species (*P. chinensis* and *P. dahurica*) based on 26,724 SNPs obtained by MIG-seq analysis (R = 0.1, genotyping rate 10%). In this tree, all Japanese populations formed a monophyletic clade with strong bootstrap support (BS = 100%), indicating a single lineage for the species within Japan. Importantly, the Jeju Island population (K3) was identified as the sister clade to the Japanese clade (BS = 98%), suggesting that the migration route into Japan likely passed through the Korean Peninsula.

The continental populations exhibited a more complex phylogenetic structure. A Chinese population (C1) was the first to diverge but did not form a distinct clade. Four Russian populations (R1, R2, R3, and R4) formed a clade, but they were not monophyletic within it, indicating potential genetic mixing or incomplete lineage sorting. Another Russian population (R5) and three Korean populations (K1, K2, and K3) each formed distinct clades with high bootstrap support (91–100%).

Within the Japanese clade, two major subclades were identified (both BS = 100 %): one

comprising eastern Japan populations (J1–J11) and the other comprising western Japan populations (J12–J23). East Japan clade was further divided into two subclades, East-1 (J7–11, BS = 83%) and East-2 (J1–6, BS = 99%), while West Japan clade consisted of two subclades, West-1 (J12–J15, J17, and J18, BS = 100%) and West-2 (J16 and J19–J23, BS = 99%).

Genetic diversity

Genetic diversity estimated for each population is shown in Table 3. A total of 667 SNPs (R = 0.5, average genotyping rate = 22.23%) from 381 individuals of 32 populations were used. The results show that the mean values of heterozygosity were relatively similar between Japanese (H_O = 0.033–0.079, av. 0.056, H_E = 0.046–0.093, av. 0.066, uH_E = 0.051–0.100, av. 0.072), Korean (H_O = 0.060–0.067, av. 0.065, H_E = 0.064–0.068, av. 0.066, uH_E = 0.069–0.075, av. 0.071), Russian (H_O = 0.034–0.068, av. 0.052, H_E = 0.031–0.088, av. 0.061, uH_E = 0.047–0.093, av. 0.067) and Chinese (H_O = 0.062, H_E = 0.061, uH_E = 0.066) populations. The mean of all populations for the inbreeding coefficient was F_{IS} = 0.094. Excessively high or low values were not detected, except for R4 in Russia (F_{IS} = –0.486).

Genetic structure of the populations

The STRUCTURE analysis was conducted using the same 667 SNPs that were used for estimating genetic diversity. From K = 2 to 6, the log likelihood of the data, LnP (K), continued to increase slightly with increasing K (Fig. 3a). Furthermore, within the same K, the values of LnP (K) showed little variation and the clustering results were stable. However, from K = 7 to 10, LnP (K) of each K showed large variations among runs and the clustering results were not stable in each K. The ΔK values, indicating the most meaningful number of K, peaked at K = 3 and 6 (Fig. 3b). At K = 2, Japanese populations and the continental populations were divided. At K = 3, genetic differentiation between the populations of eastern Japan (J1–J11, purple), western Japan (J12–J23, blue), and the continent (K1–K3, R1–R5, C1, orange) were observed. The eastern Japan group and the western Japan group corresponded to the East Japan and West Japan clades in the phylogenetic tree, respectively (Figs. 2, 3c). At K = 4, a new cluster appeared among the populations of western Japan, therefore the western Japan populations were divided into two groups which corresponded to West-1 (J12–15, J17, J18, blue), and West-2 (J16, J19–23, green), (Figs. 2, 3c). Among them, the population J15 consisted of two clusters, blue and green, and the populations J10 and J11 consisted of blue and purple. At K = 5, a new reddish purple cluster appeared in the populations J7–11, J13, and J22. However, compared to the phylogenetic tree, it was difficult to find any clear phylogenetic relationship between these populations. At K = 6, the orange cluster comprising the Korean populations (K1–3) and one Russian population (R5) corresponded to a paraphyletic grade, while the pink cluster comprising the Russian populations (R1–4) and the Chinese population (C1) corresponded to the basal paraphyletic grade (Fig. 2).

The NeighborNet network formed three groups each consisting of the continental populations, eastern Japan populations and western Japan pop-

TABLE 2. Pearson correlation coefficients for the seven climatic variables used inthe ecological nihe modeling analysis.

Variables		BIO1	BIO2	BIO3	BIO5	BIO12	BIO14	BIO15
BIO1	Annual mean temperature	-	-	-	-	-	-	-
BIO2	Mean diurnal range	-0.635	-	-	-	-	-	-
BIO3	Isothermality	0.503	0.065	-	-	-	-	-
BIO5	Max temperature of warmest month	0.761	-0.373	0.048	-	-	-	-
BIO12	Annual precipitation	0.682	-0.716	0.351	0.361	-	-	-
BIO14	Precipitation of driest month	0.411	-0.682	-0.099	0.271	0.677	-	-
BIO15	Precipitation seasonality	-0.345	0.719	0.120	-0.151	-0.549	-0.773	-

TABLE 3. Genetic diversity of each population.

Population	*N*	*N*a	*N*e	*I*	H_O	H_E	uH_E	F_{IS}
Japan								
J1	9.297	1.193	1.091	0.097	0.057	0.063	0.068	0.077
J2	8.514	1.244	1.104	0.114	0.067	0.072	0.079	0.057
J3	10.142	1.307	1.146	0.140	0.067	0.090	0.096	0.173
J4	6.180	1.186	1.089	0.094	0.058	0.061	0.068	0.035
J5	11.007	1.339	1.137	0.138	0.066	0.087	0.092	0.154
J6	9.795	1.358	1.145	0.148	0.079	0.093	0.100	0.098
J7	2.649	1.078	1.016	0.076	0.060	0.050	0.063	-0.206
J8	8.135	1.241	1.105	0.105	0.051	0.067	0.073	0.188
J9	6.913	1.156	1.070	0.079	0.056	0.051	0.056	-0.076
J10	6.118	1.135	1.064	0.071	0.036	0.046	0.051	0.121
J11	7.094	1.115	1.052	0.072	0.048	0.048	0.052	-0.016
J12	6.396	1.201	1.091	0.101	0.063	0.065	0.073	0.016
J13	12.327	1.343	1.135	0.137	0.067	0.086	0.090	0.150
J14	11.196	1.309	1.138	0.135	0.069	0.086	0.091	0.125
J15	7.459	1.319	1.147	0.144	0.063	0.092	0.099	0.222
J16	2.753	1.139	1.079	0.092	0.049	0.062	0.076	0.154
J17	8.741	1.169	1.078	0.085	0.055	0.055	0.059	0.013
J18	9.000	1.151	1.076	0.083	0.035	0.055	0.059	0.259
J19	11.361	1.138	1.072	0.073	0.033	0.048	0.051	0.230
J20	8.924	1.150	1.074	0.078	0.044	0.051	0.055	0.114
J21	9.430	1.190	1.095	0.089	0.055	0.058	0.063	0.019
J22	12.132	1.250	1.115	0.110	0.051	0.071	0.074	0.234
J23	6.852	1.202	1.097	0.096	0.065	0.062	0.068	-0.045
Avarage	8.366	1.214	1.096	0.102	0.056	0.066	0.072	0.091
South Korea								
K1	8.175	1.220	1.109	0.105	0.067	0.068	0.075	0.017
K2	7.777	1.193	1.095	0.099	0.067	0.065	0.070	-0.036
K3	7.667	1.207	1.103	0.099	0.060	0.064	0.069	0.035
Avarage	7.873	1.207	1.102	0.101	0.065	0.066	0.071	0.006
Russia								
R1	1.255	0.853	0.836	0.044	0.046	0.031	0.047	-0.486
R2	12.141	1.228	1.108	0.101	0.050	0.066	0.069	0.165
R3	11.979	1.160	1.070	0.073	0.034	0.047	0.049	0.212
R4	10.681	1.318	1.141	0.138	0.061	0.088	0.093	0.215
R5	12.313	1.301	1.109	0.121	0.068	0.075	0.079	0.067
Avarage	9.674	1.172	1.053	0.096	0.052	0.061	0.067	0.035
China								
C1	8.414	1.183	1.070	0.096	0.062	0.061	0.066	-0.008
Total Avarage	8.526	1.206	1.089	0.101	0.057	0.065	0.071	0.094

N = number of genotypes
*N*a = number of different alleles
*N*e = number of effective alleles = 1 / (Sum pi^2)
I = Shannon's information index = -1* Sum (pi * Ln (pi))
H_O = observed heterozygosity = number of *H*ets / *N*
H_E = expected heterozygosity = 1 - Sum pi^2
uH_E= unbiased expected heterozygosity = (2*N* / (2*N*-1)) * H_E
F_{IS} = fixation index = (H_E - H_O) / H_E = 1 - (H_O / H_E)
Where pi is the frequency of the ith allele for the population & Sum pi^2 is the sum of the squared population allele frequencies.

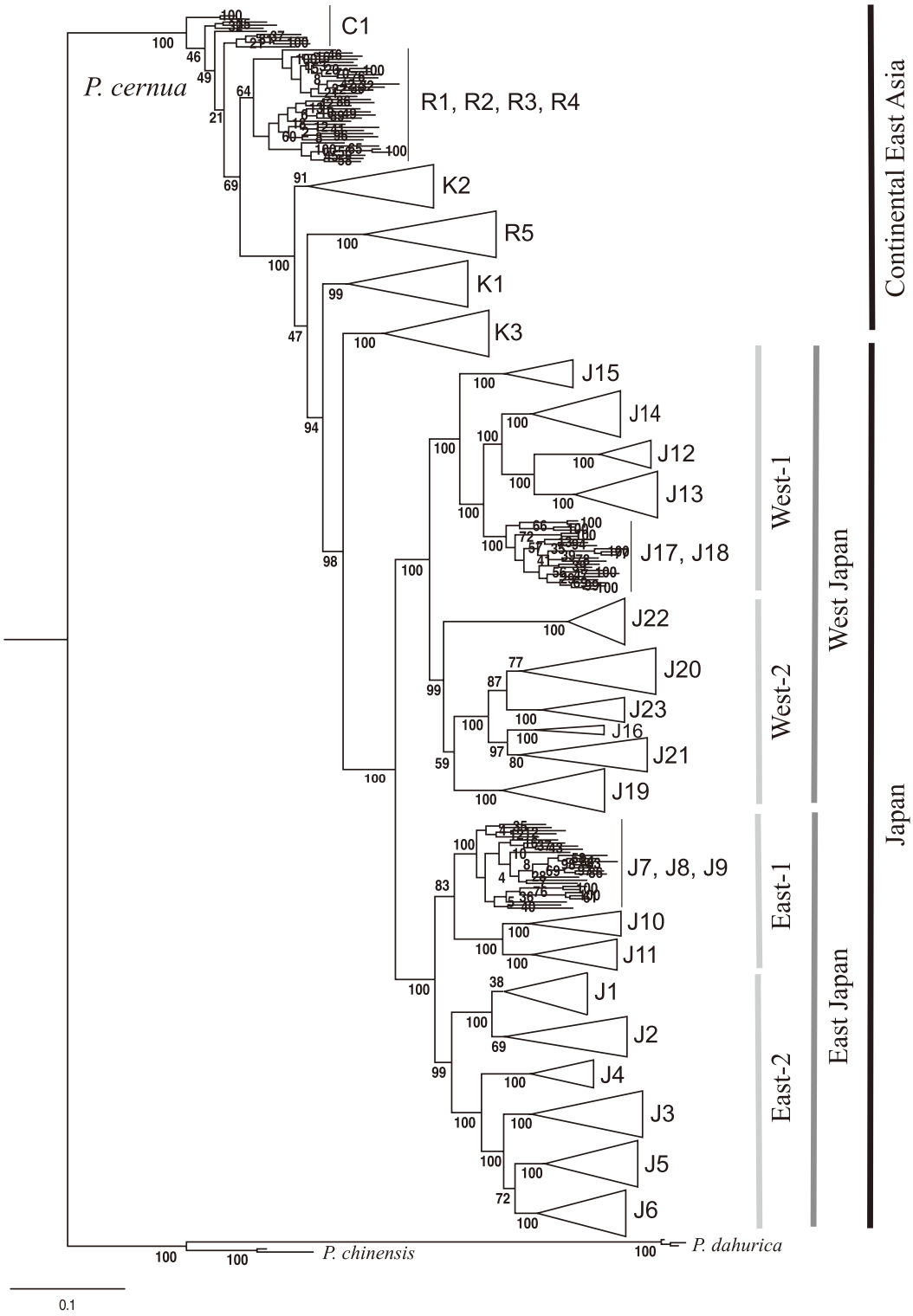

FIG. 2. Phylogenetic tree based on the maximum likelihood (ML) analysis among populations of *Pulsatilla cernua* using SNP data obtained by MIG-seq analysis. Numbers along branches indicate bootstrap probabilities (%) based on 1000 replicates.

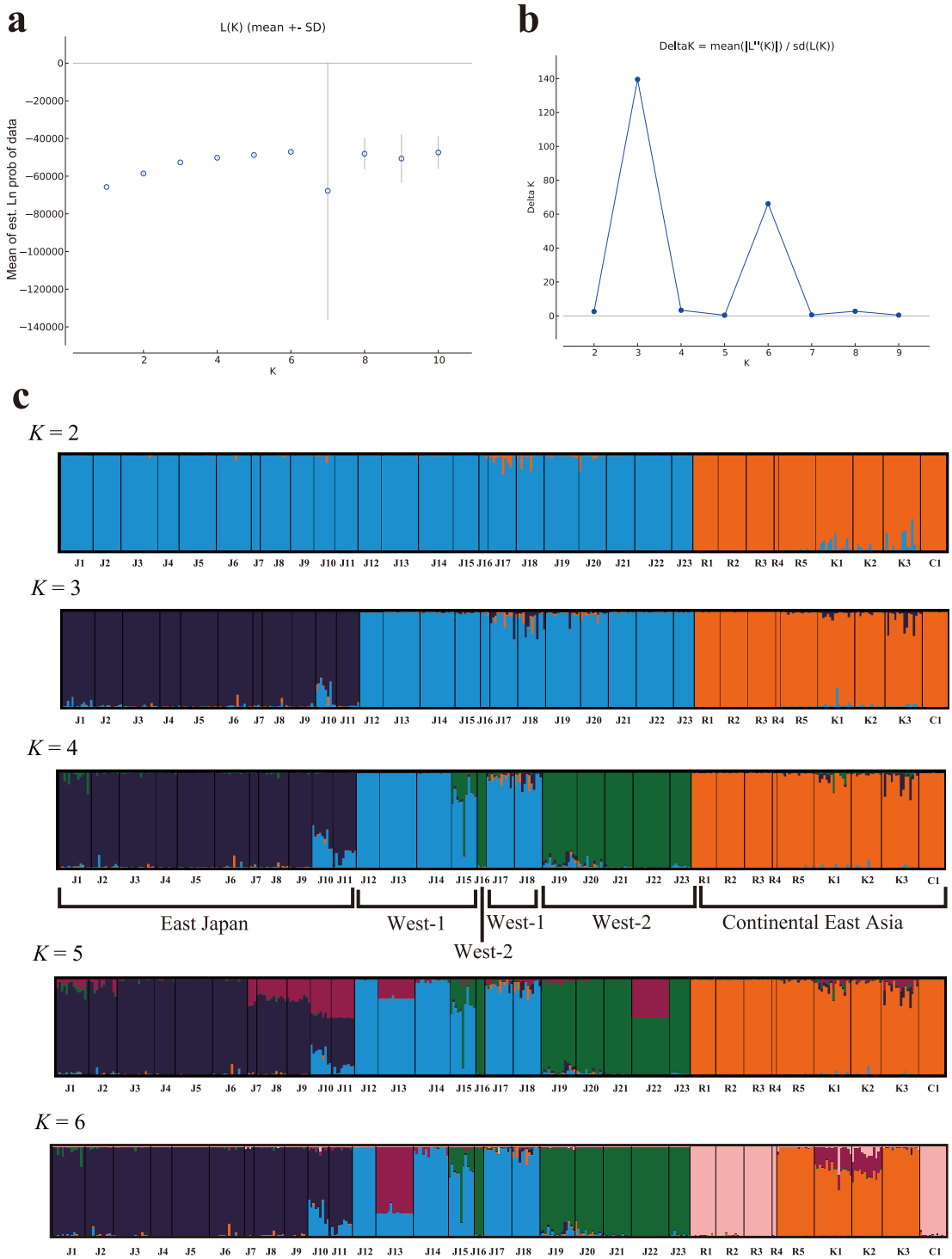

FIG. 3. Result of Bayesian clustering analyses in STRUCTURE on *Pulsatilla cernua*. **a**, Mean L (K) ± SD over 10 runs. **b**, Plots of delta-K values against $K = 2$–10. **c**, bar plots show estimated probabilities of ancestral clusters of each sample. Populations and their geographic areas are shown below bar plot.

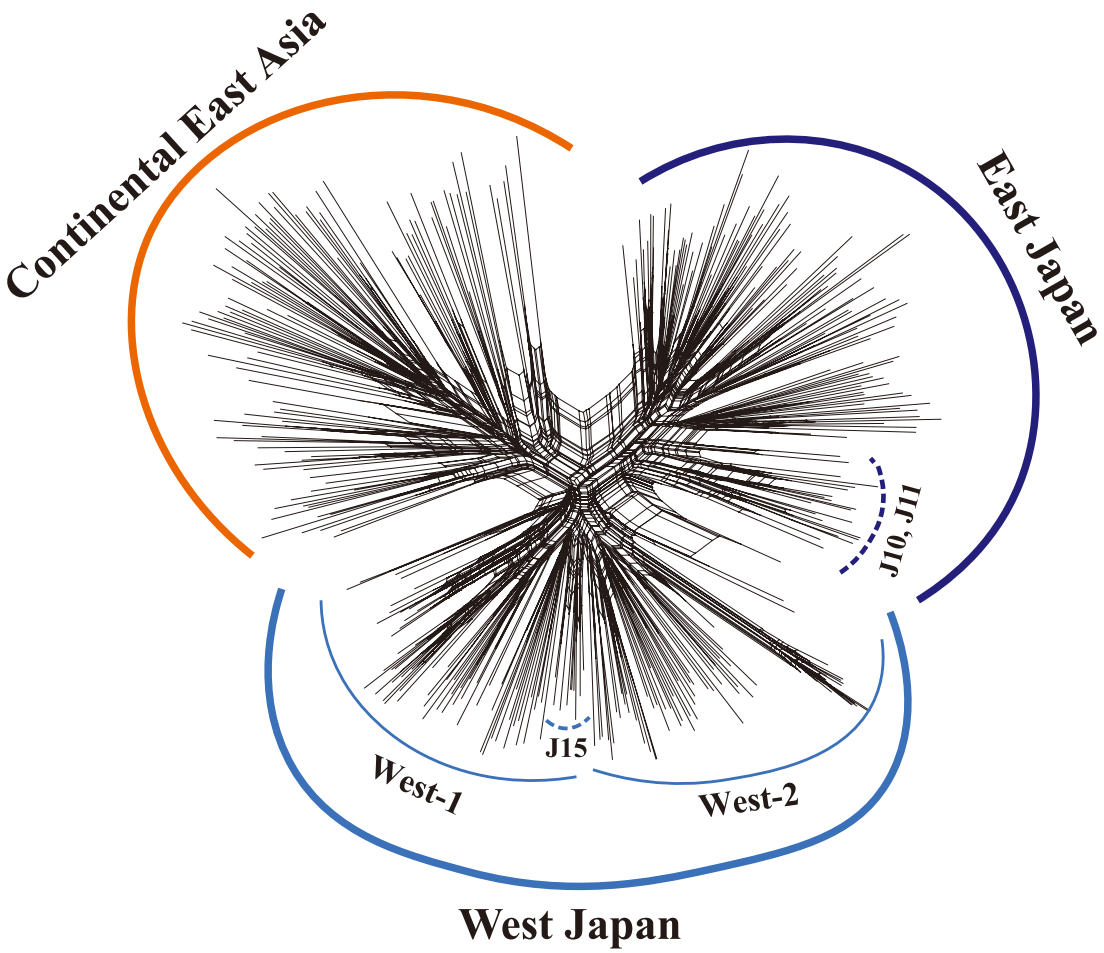

FIG. 4. NeighborNet dendrogram of 32 populations of *Pulsatilla cernua*. Three groups, Continental East Asia, western Japan, and eastern Japan, and two subgroups, West-1 and West-2 correspond to clades and subclades in Figure 2.

ulations (Fig. 4). The three clusters corresponded to the three groups observed in $K = 3$ of the STRUCTURE analysis (Fig. 3). While not strictly so, each population formed its own cluster. The population of J10 and J11 were located between the groups of eastern Japan and western Japan; population 15 was located between West-1 and West-2.

DIYABC analysis

The DIYABC analysis was performed in three steps, DIYABC-1, DIYABC-2, and DIYABC-3 (Fig. 5). Posterior probability and its 95% confidence interval based on the logistic estimate are shown in Table 4. In the DIYABC-1, Scenario 2 obtained the highest posterior proba-

TABLE 4. Posterior probability of each scenario and its 95% confidence interval based on the logistic estimate.

Sceneario	Posterior probability	95% CI
DIYABC 1		
Scenario 1	0.295	0.264-0.327
Scenario 2	0.476	0.442-0.509
Scenario 3	0.229	0.202-0.256
DIYABC 2		
Scenario 1	0.023	0.015-0.031
Scenario 2	0.081	0.053-0.108
Scenario 3	0.896	0.866-0.927
DIYABC 3		
Scenario 1	0.489	0.462-0.516
Scenario 2	0.080	0.055-0.106
Scenario 3	0.429	0.400-0.458
Scenario 4	0.002	0.000-0.029

bility (0.476, 95% CI 0.442–0.509). This scenario suggests that the populations of eastern Japan were divided from the populations of western Japan after migration from the continent. In the DIYABC-2, Scenario 3 obtained the highest posterior probability (0.896, 0.866–0.927), which means that the populations of West-1 were separated from the populations of West-2 after segregation between East and West. The three populations (J10, J11, and J15), presumed to be of hybrid origin, were included in the analysis of DIYABC-3 to infer time and order of hybridization events. Posterior probabilities of Scenarios 1 (0.489, 0.462–0.516) and 3 (0.429, 0.400–0.458) were much higher than those of Scenarios 2 (0.080, 0.055–0.106) and 4 (0.002, 0.000–0.029), with a slightly higher value of the Scenario 1. Scaled demographic parameters estimated are shown in Table 5.

Pulsatilla cernua is a perennial species. Although the generation time of *P. cernua* has not been clearly determined, it may take several years for anthesis after germination, as we observed young, sterile individuals of various sizes even during the flowering season. Therefore, we assumed three years as a generation time of *P. cernua*. The scaled divergence times of t1 (divergence between West Japan and East Japan) and t2 (divergence between the continent and Japan) in the scenario2 of the DIYABC-1 analysis were 30,900 (95% CI 15,420–43,200) and 35,100 (11,580–58,200) ya; t1 (divergence between West-1 and West-2), t2 (divergence between West Japan and East Japan), and t3 (divergence between the continent and Japan) in Scenario 3 of the DIYABC-2 analysis were 10,170 (5,340–14,340), 11,400 (6,510–16,110), and 13,740 (4,800–26,760); in Scenario 1 of the DIYABC-3 analysis, t1 (hybridization between West-1 and East Japan), t2 (hybridization between West-1 and West-2), t3 (divergence between West-1 and West-2), t4 (divergence between West Japan and East Japan), and t5 (divergence between the continent and Japan) were 13,500 (4,980–20,040), 12,930 (7,560-18,780), 14,040 (8,790–20,910), 20,640 (14,640–25,680), and 29,040 (24,030–29,940); in the Scenario 3 of the DIYABC-3 analysis, t1 (hybridizations between West-1 and West-2, and West-1 and East Japan), t2 (divergence between West-1 and West-2), t3 (divergence between West Japan and East Japan), and t4 (divergence between the continent and Japan) were 12,810 (6,810–18,360), 25,110 (19,200–28,740), 28,860 (23,940–29,940), and 44,700 (27,120–56,100) (Table 5).

Ecological niche modelling

The average test AUC of the MaxEnt model was 0.952, indicating a high level of predictive accuracy (Swets 1988, Pearce & Ferrier 2000). The confusion matrix was calculated using the 10% logistic threshold value of 0.29, determined during the MaxEnt analysis. This threshold classified areas as suitable or unsuitable habitats in the present climate model. The confusion matrix revealed 9,025 true negatives, 975 false positives, 4 false negatives, and 61 true positives. Based on these values, the omission error rate, representing the percentage of true presence points incorrectly predicted as absences, was 6.2%, while the commission error rate, representing the percentage of pseudo-absence points incorrectly predicted as presences, was 9.8%. Additional evaluation metrics derived from the confusion matrix included an accuracy of 90.3%, a sensitivity of 93.8%, and a precision of 5.9%. The high sensitivity highlights the model's effectiveness in identifying true presence locations, minimizing omission errors. However, the low precision and corresponding F1-score (0.111) reflect a high rate of commission errors, which likely result from the inclusion of true presence locations within the pseudo-absence data—an inherent limitation of MaxEnt modeling. Since MaxEnt relies on pseudo-absence rather than true absence data, these limitations are unavoidable. Despite this limitation, the model's high sensitivity makes it a valuable tool for identifying potential habitats. However, these results should be interpreted with caution, considering the potential for over-prediction inherent in pseudo-absence-based models.

The percent contribution and permutation importance of the environmental variables influencing the distribution of *P. cernua* are summarized in Table 6. Among the variables, precipitation of

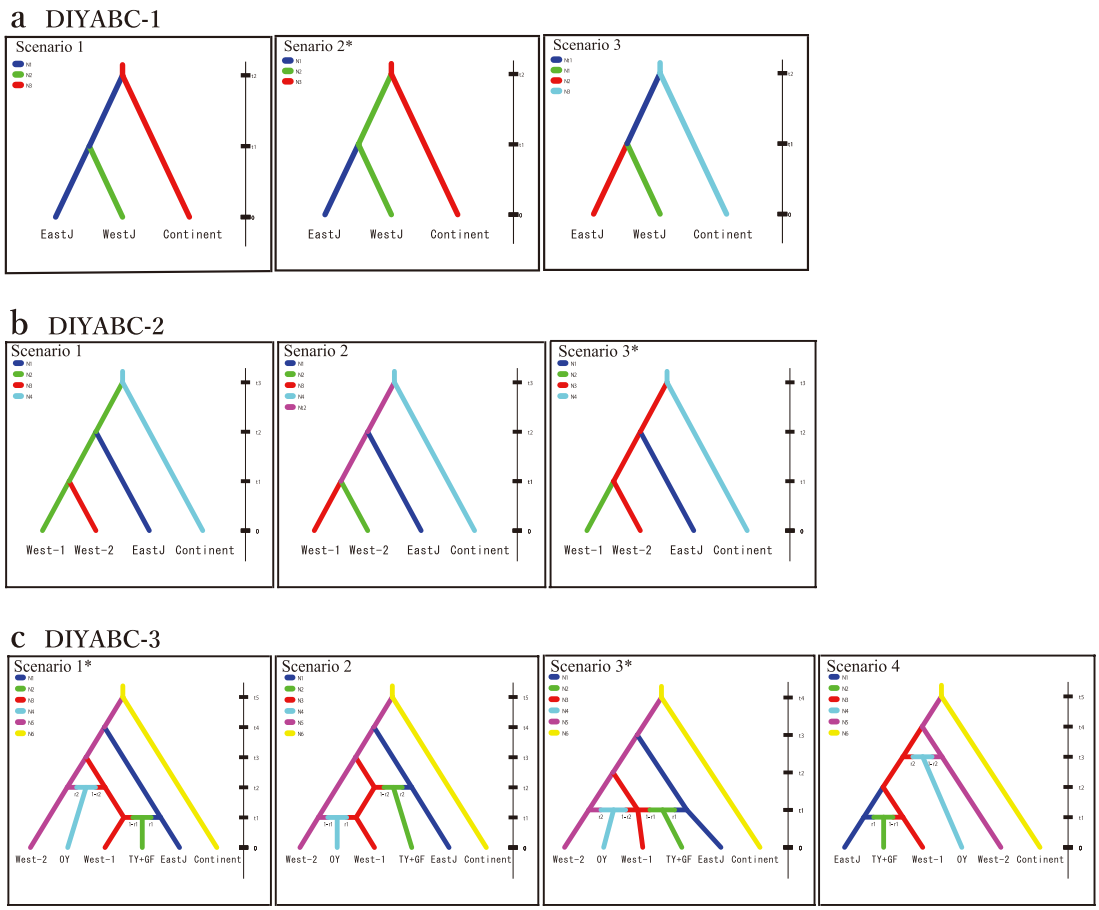

FIG. 5. Scenarios designed for inferring population demographic histories of *Pulsatilla cernua* using three steps of DIYABC analysis. **a**, DIYABC-1, included three groups, Continental East Asia, western Japan, and eastern Japan. Scenario 2* obtained highest posterior probability (PP). **b**, DIYABC-2, included four groups, Continental East Asia, West-1, West-2, and eastern Japan. Scenario 3* obtains the highest PP. **c**, DIYABC-3, included six groups, Continental East Asia, West-1, West-2, eastern Japan, J15 (OY: Okayama population), and J10+J11 (TY+GF: Toyama and Gifu populations). Scenarios 1* and 3* obtain similarly high PP.

the driest month (BIO14) showed the highest percent contribution (43.72%) and permutation importance (26.96%), indicating its critical role in shaping the species' distribution. Annual mean temperature (BIO1) was the second most important variable, contributing 33.17% to the model and having a permutation importance of 32.85%. Max temperature of the warmest month (BIO5) also exhibited a notable influence, particularly in permutation importance (26.72%). Other variables, such as annual precipitation (BIO12) and isothermality (BIO3), had relatively lower contributions but still played a role in the model. These results highlight the dominant role of climatic factors, particularly precipitation and temperature, in determining the suitable habitat for *Pulsatilla cernua*.

Based on the present distribution plotted with herbarium specimens, areas suitable for *P. cernua* at present, MID, LGM and LIG, were predicted using ENM analysis (Fig. 6). The predicted suitable areas for the current climate (10% logistic threshold: 0.29) were not substantially different from the distribution range of the herbarium specimens, except that they were predicted to be present in Hokkaido, Japan (Fig. 6b). During the LIG, the Korean Peninsula and the Japanese Archipelago from Kyushu to Hokkaido were in-

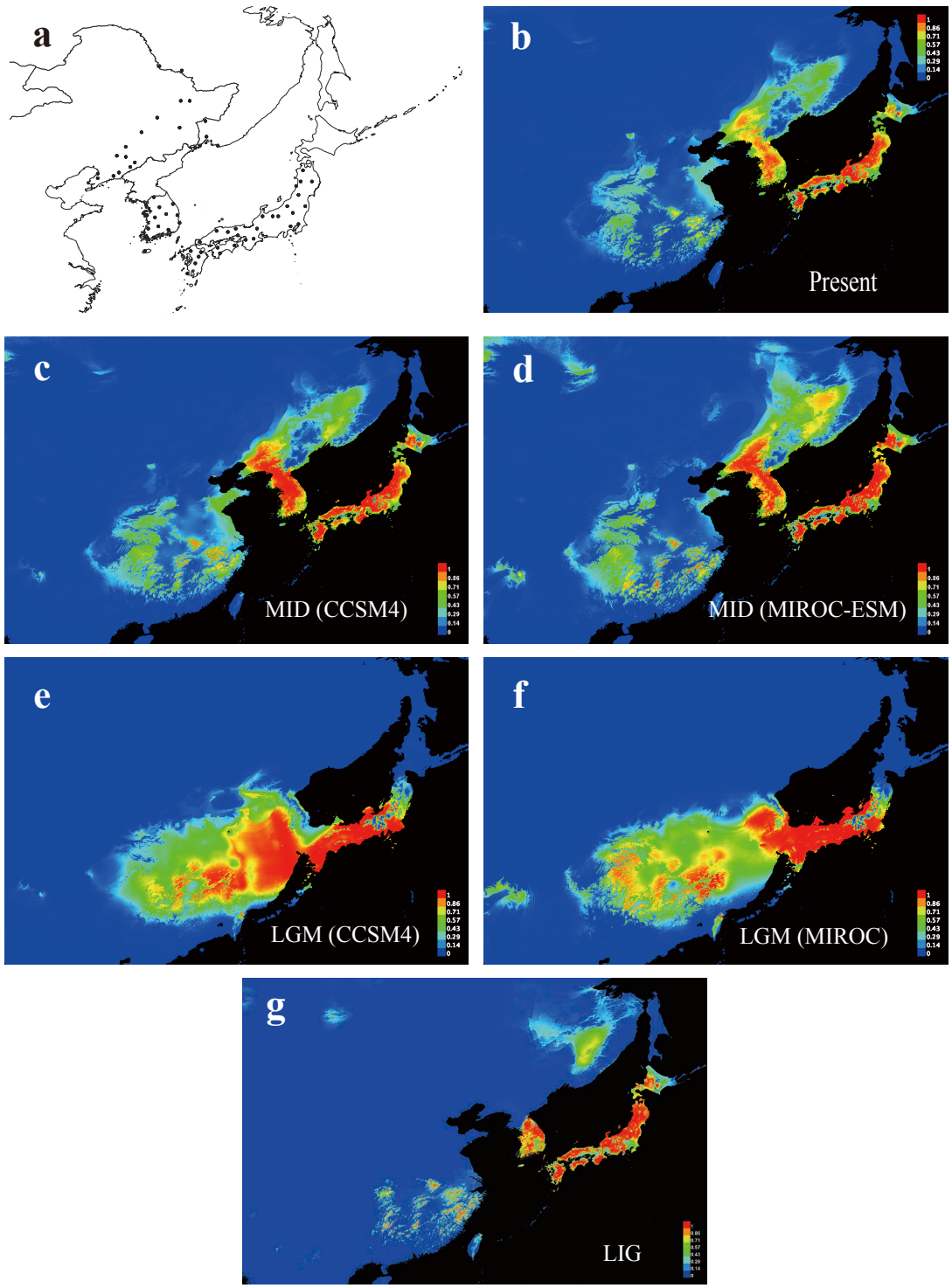

FIG. 6. Inferred potential areas for *Pulsatilla cernua* predicted by ecological niche modeling (ENM) using seven climate variables. **a**, occurrence points used for modeling. **b**, present time based on Otto-Bliesner *et al.* (2006). **c**, Middle Holocene (MID, 6000 ya) based on Community Climate System Model (CCSM4). **d**, MID based on Model for Interdisciplinary Research on Climate (MIROC). **e**, Last Glacial Maximum (LGM, 22 ka) based on the CCSM4. **f**, LGM based on the MIROC, **g**, Last Interglacial Period (LIG, 120–140 ka) based on Otto-Bliesner *et al.* (2006).

TABLE 5. Scaled demographic parameters estimated in DIYABC-1, 2, and 3

Parameter		Mean	Median	Mode	Quantile 2.5%	Quantile 97.5%
Scinario 2 in DIYABC-1						
Effectie population size	N1	29,200	29,500	31,100	16,400	40,600
	N2	24,100	23,300	23,600	6,600	46,700
	N3	37,600	38,700	39,200	22,200	47,700
Time scale in generations	t1	10,200	10,300	10,300	5,140	14,400
	t2	11,800	11,700	9,740	3,860	19,400
Time scale in years	t1*3	30,600	30,900	30,900	15,420	43,200
(3 years per generation)	t2*3	35,400	35,100	29,220	11,580	58,200
Scenario 3 in DIYABC-2						
Effectie population size	N1	7,300	7,440	7,540	4,460	9,540
	N2	6,270	6,290	6,260	3,090	9,410
	N3	7,310	7,510	7,860	3,830	9,790
	N4	25,200	24,800	22,400	11,800	40,900
Time scale in generations	t1	3,340	3,390	3,490	1,780	4,780
	t2	3,790	3,800	3,620	2,170	5,370
	t3	4,730	4,580	4,990	1,600	8,920
Time scale in years	t1*3	10,020	10,170	10,470	5,340	14,340
(3 years per generation)	t2*3	11,370	11,400	10,860	6,510	16,110
	t3*3	14,190	13,740	14,970	4,800	26,760
Scenario 1 in DIYABC-3						
Effective population size	N1	17,300	17,200	16,600	10,700	25,200
	N2	6,540	6,740	7,590	2,770	9,340
	N3	14,900	14,500	14,200	6,100	25,800
	N4	3,870	3,550	3,100	1,130	8,680
	N5	11,400	11,100	10,800	6,530	19,300
	N6	27,600	27,200	28,300	18,200	40,000
Time scale in generations	t1	4,450	4,500	4,600	1,660	6,680
	t2	4,340	4,310	4,630	2,520	6,260
	t3	4,740	4,680	4,810	2,930	6,970
	t4	6,830	6,880	7,150	4,880	8,560
	t5	9,510	9,680	9,920	8,010	9,980
Admixture rate	r1	1.47	1.52	1.67	0.73	1.97
	r2	1.50	1.58	1.94	0.41	1.98
Time scale in years	t1*3	13,350	13,500	13,800	4,980	20,040
(3 years per generation)	t2*3	13,020	12,930	13,890	7,560	18,780
	t3*3	14,220	14,040	14,430	8,790	20,910
	t4*3	20,490	20,640	21,450	14,640	25,680
	t5*3	28,530	29,040	29,760	24,030	29,940
Scenario 3 in DIYABC-3						
Effective population size	N1	14,600	14,300	13,400	7,980	24,100
	N2	4,870	4,840	5,120	1,860	8,280
	N3	15,800	15,600	16,100	7,450	26,500
	N4	3,890	3,650	2,990	1,080	8,260
	N5	12,000	11,700	11,500	6,530	20,900
	N6	43,900	44,600	45,700	34,200	49,300
Time scale in generations	t1	4,250	4,270	3,840	2,270	6,120
	t2	8,260	8,370	8,480	6,400	9,580
	t3	9,460	9,620	9,940	7,980	9,980
	t4	14,700	14,900	15,600	9,040	18,700
Admixture rate	r1	0.96	0.89	0.79	0.28	1.92
	r2	0.63	0.51	0.24	0.06	1.80
Time scale in years	t1*3	12,750	12,810	11,520	6,810	18,360
(3 years per generation)	t2*3	24,780	25,110	25,440	19,200	28,740
	t3*3	28,380	28,860	29,820	23,940	29,940
	t4*3	44,100	44,700	46,800	27,120	56,100

TABLE 6. Average percent contribution and permutation importance of environmental variables influencing the distribution of *Pulsatilla cernua*.

Variables	Percent contribution (%)	Permutation importance (%)
Annual mean temperature (BIO1)	33.17	32.85
Mean diurnal range (BIO2)	1.22	0.15
Isothermality (BIO3)	0.8	1.61
Max temperature of warmest month (BIO5)	13.06	26.72
Annual precipitation (BIO12)	6.59	11.23
Precipitation of driest month (bio14)	43.72	26.96
Precipitation seasonality (bio15)	1.44	0.48

dicated to be suitable areas, while the area was rather restricted on the continent (Fig. 6g). The potential distributions during the LGM were slightly discordant between the climate models; that is, the CCSM4 predicted strong probability in southeastern China (Fig. 6e) than did the MIROC (Fig. 6f). On the other hand, both models are coincident that the potential range cover is in Kyushu, Shikoku, and almost all of Honshu in Japan. Both models were similar in the suitable areas at the MID (ca. 6000 ya), in which the areas in China were smaller than those in the LGM while the areas in Japan and Russia were enlarged toward the north (Fig. 6c, d).

Discussion

Origin and migration route of the Japanese populations of Pulsatilla cernua

The phylogenetic tree based on MIG-seq analysis showed that all Japanese populations of *Pulsatilla cernua* formed a clade which was sister to the clade of Jeju Island (K3) (Fig. 2). Although most continental populations formed distinct clades, the Russian populations (R1-4) formed a mixed clade. The limited number of sampled populations from the continent, particularly from China, prevent us from fully elucidating the phylogeographic history on the continent. However, the results showed that the Jeju population was sister to the Japanese clade and the Russian R5 and the Korean K1 and K2 formed a sister grade to the Japan-Jeju clade. This supported the continental origin of *P. cernua* and its migration route via Korean Peninsula.

Genetic structure of the Japanese populations of Pulsatilla cernua

The STRUCTRE analysis and NeighborNet analysis revealed that three groups, Continental East Asia, western Japan, and eastern Japan, are genetically distinct in *P. cernua* (Figs. 3 & 4). The two Japanese groups correspond to the two clades, West Japan and East Japan, which are further divided into two subclades, West-1 and West-2, and East-1 and East-2, as shown in the phylogenetic tree (Fig. 2). The STRUCTURE analysis indicated genetic differentiation between West-1 and West-2 at $K = 4$ (Fig. 3). Since genetic differentiation between East-1and East-2 was ambiguous, it is feasible to recognize three genetically differentiated groups that were at least once isolated from each other in Japan in the past. As for the genetic structure within the three groups in Japan, each population showed genetic similarity among individuals, but a few populations (J10, J11, and J15) possessed a genetically mixed structure as follows. According to the bar-plots of the STRUCTURE analysis at $K = 4$, most individuals in populations J10 and J11 consisted of the eastern Japan cluster (purple) and the West-1 cluster (blue), while the individuals of J15 consisted of the West-1 cluster (blue) and the West-2 cluster (green). Additionally, in the Neighbor-Net analysis, the J10 and J11 populations were located between eastern Japan and western Japan, while J15 was between West-1 and West-2 (Fig. 4). Consid-

ering the geographic position of the populations shown in Figure 1, it is likely that they resulted from hybridization between eastern Japan and West-1 and West-1 and West-2, respectively.

Although Takaishi *et al.* (2019) suggested the possibility that *Pulsatilla cernua* maintained a continuous distribution until recently based on chloroplast DNA haplotype data, the results obtained in this study indicate that three geographically isolated population groups once existed in Japan. This discrepancy can be attributed to the difference in the rates of evolution between nuclear and chloroplast genomes. Since the chloroplast genome evolves more slowly than the nuclear genome (Wolfe *et al.* 1987, Taberlet *et al.* 2007), even if sufficient time has passed for nuclear genome differentiation, it may still be too short for chloroplast genome differentiation. As a result, genetic structure may arise in the nuclear genome, while the chloroplast genome remains homogeneous.

Divergence time and phylogeographic history of Pulsatilla cernua

According to the results of the DIYABC analysis, East Japan was derived from the West Japan, and West-1 was derived from West-2 (Fig. 5a, b & Table 4). In the analysis of DIYABC-3, the posterior probabilities for Scenario 1 and Scenario 3 were almost identical (0.489 for Scenario 1 and 0.429 for Scenario 3, Table 4), which means that hybridization between East Japan and West Japan and hybridization between West-1 and West-2 occurred almost simultaneously.

The scaled divergence time estimated for the four highly supported scenarios (Scenario 2 in the DIYABC-1, Scenario 3 in the DIYABC-2, and Scenarios 1 and 3 in the DIYABC-3) indicated that the Japanese populations diverged from continental populations 13,740–44,700 (total range 4,800–58,200) ya. Although it should be noted that the age estimates did not fully converge and that the generation time used for divergence time estimation remains uncertain, it is likely that migration to Japan occurred during the middle to late LGP. The ENM analysis indicated that most of the Japanese Archipelago was suitable for *P. cernua* in the LIG (Fig. 6g). Although the suitable area has been decreasing, it remained relatively extensive in the western part of Japan under the cooling climate towards the LGM (Fig. 6e, f). While the estimated range is not well constrained, this inference coincides with the timing of migration hypothesized to have occurred in the late Pleistocene (Kitamura 1957, Hotta 1974, Murata 1977, 1988, Tabata 1997). The divergence times between East Japan and West Japan, as well as between West-1 and West-2, were estimated as 11,400–30,900 (total range 6,510–43,200) ya and 10,170–25,110 (total range 5,340–28,740) ya, respectively. These estimates suggest that *P. cernua* once expanded into eastern Japan before the LGM and subsequently divided into three regions during the coldest period of the LGM. The larger genetic differentiation between East and West Japan than between West-1 and West-2 (Fig. 3) support the earlier separation of East Japan and West Japan as shown in the phylogenetic tree (Fig. 2). The ENM results indicate the possibility that refugia existed in the southern part of eastern Japan even during the LGM. After the LGM, range expansion under a warming climate facilitated contact between these groups, leading to hybridization among them. The hybridizations were supposed to have occurred between 12,810–13,500 (4,980–20,040) ya by the Scenarios 1 and 3 of the DIYABC-3.

Phylogeographic history of Pulsatilla cernua *as one of the Mansen elements*

The Mansen elements are sometimes referred to as ‘continental-grassland relicts’ because they inhabit semi-natural grasslands that emerged after the decline of natural grasslands following the LGM (Tabata 1997, Murata 1988, Ushimaru *et al.* 2018). However, each species may have experienced a distinct demographic history. Previous studies on the Mansen elements have supported a continental origin and migration to Japan during the LGP for *Viola orientalis* (Sata *et al.* 2021), *Potentilla discolor* (Fujii *et al.* 2025), and *Tephroseris kirilowii* (Sakaba *et al.* 2023). A migration route via the Korean Peninsula has been identified for *V. orientalis*. In the case of *P. cernua*,

consistent with other Mansen elements, the present phylogenetic analysis indicated that *Pulsatilla cernua* originated in continental East Asia and migrated to the Japanese Archipelago via the Korean Peninsula during the LGP.

However, historical inferences regarding subsequent range shifts within the Japanese Archipelago are not consistent among species. The genetic structure of *Viola orientalis* (Sata *et al.* 2021) and *P. discolor* (Fujii *et al.* 2025) suggest that their populations in Japan were once separated following an initial range expansion. In contrast, the low genetic divergence among populations of *Thefroseris kirilowii* (Sakaba *et al.* 2023) and *Geranium krameri* (Kurata *et al.* 2023) suggests a single expansion and/or a continuous gene flow among populations. For *P. cernua*, our analyses revealed its historical range shift in greater detail. After an initial expansion that possibly extended into eastern Japan, the populations were subsequently divided into West Japan and East Japan, and further subdivided into West-1 and West-2, and East-1 and East-2, respectively. Evidence of hybridization between West Japan and East Japan, as well as between West-1 and West-2 indicates that secondary range expansions brought those separated populations back into contact. This represents the first documented case among the Mansen elements in which previously fragmented distribution ranges have come into secondary contact through subsequent range expansion.

Grassland-associated Mansen elements are considered to have become relict in Japan due to the reduction of grasslands caused by postglacial warming (Murata 1988, Tabata 1997, Ushimaru *et al.* 2018). However, post-LGM range expansion, possibly associated with the spread of semi-natural grasslands, was suggested for *P. cernua* and *T. kirilowii*. Furthermore, range fragmentation following an initial expansion was suggested for *P. cernua*, *V. orientalis*, and *P. discolor*, whereas either a single expansion event or continuous gene flow was inferred for *T. kirilowii* and *G. krameri*. These findings elucidate the diverse demographic histories of the Mansen elements, which may have been shaped by their intrinsic biological traits— such as growth habit, seed dispersal mechanisms, and differences in temperate and/or moisture requirements—as well as the timing or their migration to Japan. To further elucidate the history of grasslands, which are important components of Japanese vegetation, phylogenetic analyses of additional Mansen elements are necessary.

We would like to express our cordial thanks to the following persons to their kind help in collecting samples. Kenichi Hashiba, Masashi Igari, Yasuhiko Inoue, Hitoshi Iwamura, Kosuke Kato, Takayuki Kawahara, Satoru Kinoshita, Tsuzuki Miyagawa, Fumio Mototani, Naoyuki Nakahama, Shuichi Nemoto, Jun Nishihiro, Yoko Oota, Masataka Otomasu, Tomoka Sakaba, Takeshi Sato, Kazuhiro Sawa, Sumio Sei, Fujio Suzaki, Mitsuko Suzaki, Hiroshi Takahashi, Asuka Takaishi, Kenta Tanaka, Kazuhiko Uchinuno, Masato Watanabe, and Naruyo Yamada in Japan, Jiahao Chen in China and Jungsim Lee in South Korea (honorifics omitted, in alphabetical order). This research was supported by JSPS KAKENHI Grant Number JP17H03721 and a grant from the Institute of Plant Science and Resources, Okayama University (3037, 3140, and R236).

References

Bolger, A. M., M. Lohse, & B. Usadel. 2014. Trimmomatic: A flexible trimmer for Illumina sequence data. Bioinformatics 30: 2114–2120.

Boria, R. A., L. E. Olson, S. M. Goodman & R. P. Anderson. 2014. Spatial filtering to reduce sampling bias can improve the performance of ecological niche models. Ecol. Model. 275: 73–77.

Bradbury, P. J., Z. Zhang, D. E. Kroon, T. M. Casstevens, Y. Ramdoss & E. S. Buckler. 2007. TASSEL: software for association mapping of complex traits in diverse samples. Bioinformatics 23: 73–77.

Bryant, D. & V. Moulton. 2004. Neighbor-bet: and agglomerative method for the construction of phylogenetic networks. Mol. Biol. Evol. 21: 255–265.

Catchen, J., A. Amores, P. Hohenlohe, W. Cresko & J. H. Postlethwait. 2011 Stacks: building and genotyping loci *de novo* from short-read sequences. G3 1: 171–182.

Cornuet, J.-M, P. Pudlo, J. Veyssier, A. Dehne-Garcia, M. Gautier, R. Leblois, J.-M. Marin & A. Estoup. 2014. DIYABC v2.0: a software to make approximate Bayesian computation inferences about population history using single nucleotide polymorphism, DNA sequence and microsatellite. Bioinformatics 30: 1187–

1189.
Doyle, J. J. & J. L. Doyle. 1987. A rapid DNA isolation procedure for small quantities of fresh leaf tissue. Phytochem. Bull. 19: 11–15.
Earl, D. A. & B. M. von Holdt. 2012. Structure Harvester: a website and program for visualizing Structure output and implementing the Evanno method. Conservation Genetics Resources 4: 359–361.
Evanno, G., S. Regnaut & J. Goudet. 2005. Detecting the number of clusters of individuals using the software STRUCTURE: a simulation study. Mol. Ecol. 14: 2611–2620.
Fourcade, Y., J. O. Engler, R. Dennis & J. Secondi. 2014. Mapping species distributions with MAXENT using a geographically biased sample of presence data: a performance assessment of methods for correcting sampling bias. PLOS One 9: e97122.
Fujii, N., H. Kobatake, K. Niki, R. Taira, T. Iwasaki, H. Ikeda, Y. Suyama, A. Matsuo, K. Takeshita, A. E. Kozhevnikov, Z. V. Kozhevnikova, H. -T. Im, J. -H. Pak, K. Choi, H. Wang, T. -G. Gao, H. Wang, S. Wang & A. Soejima. 2025. Phylogeography of *Potentilla discolor* (Rosaceae), a temperate grassland species, around the Japanese Archipelago. Acta Phytotax. Geobot. 76: 85–109.
Gent, P. R., G. Danabasoglu, L. J. Donner, M.M. Holland, E. C. Hunke, S. R. Jayne, D. M. Lawrence, R. B. Neale, P. J. Rasch, M. Vertenstein, P. H. Worley, Z.-L. Yang & M. Zhang. 2011. The community climate system model version 4. J. Climate 24: 4973–4991.
Hedrick, P. W. 2005. A standardized genetic differentiation measure. Evolution 59: 1633–1638.
Hijmans, R. J., S. E. Cameron, J. L. Parra, P. G. Jones & A. Jarvis. 2005. Very high resolution interpolated climate surfaces for global land areas. Int. J. Climatol. 25: 1965–1978.
Hotta, M. 1974. History and Geography of Plants. Sanseido, Tokyo (in Japanese).
Huson, D. H. & D. Bryant. 2006. Application of phylogenetic networks in evolutionary studies. Mol. Biol. Evol. 23: 254–267.
Jost, L. 2008. GST and its relatives do not measure differentiation. Mol. Ecol. 17: 4015–4026.
Kawano, T., N. Sakai, T. Hayashi & H. Takahara. 2012. Grassland and fire history since the late-glacial in northern part of Aso Caldera, central Kyushu, Japan, inferred from phytolith and charcoal records. Quat. Int. 254: 18–27.
Kitamura, S. 1957. Distribution of plants. *In*: Kitamura, S., G. Murata & M. Hori (eds.), Coloured Illustrations of Herbaceous Plants of Japan I, pp. 246–264. Hoikusha, Osaka (in Japanese).
Koidzumi, G. 1931. Zengen. *In*: Maebara, K. (ed.) Florula Austro-Higensis, pp. xv–xviii. Sanshusha, Tokyo (in Japanese).
Kopelman, N. M., J. Mayzel, M. Jakobsson, N. A. Rosenberg & I. Mayrose. 2015. Clumpal: a program for identifying clustering modes and packaging population structure inferences across K. Mol. Eco. Resou. 15: 1179–1191.
Kurata, S., S. Sakaguchi, S. K. Hirota, O. Kurashima, Y. Suyama & M. Ito. 2024. Phylogeographic incongruence between two related species with divergent habitat preferences in East Asia. Ecol. Res. 39: 273–88.
Leaché, A. D., B. L. Banbury, J. Felsenstein, A. N. de Oca & A. Stamatakis. 2015. Short tree, long tree, right tree, wrong tree: new acquisition bias corrections for inferring SNP phylogenies. Syst. Biol. 64: 1032–1047.
Lee, Y. N. 1967. Chromosome numbers of flowering plants in Korea. J. Korean Res. Inst. Ewha Women's Univ. 11: 455–478.
Meirmans, P. G. & P. W. Hedrick. 2011. Assessing population structure: F_{ST} and related measures. Mol. Ecol. Resour. 11: 5–18.
Meirmans, P. G. & P. H. Tienderen. 2004. GenoType and GenoDive: two programs for the analysis of genetic diversity of asexual organisms. Mol. Ecol. Notes 4: 792–794.
Ministry of the Environment of Japan. 2016. Japan Biodiversity Outlook 2: Report of Comprehensive Assessment of Biodiversity and Ecosystem Services in Japan. Nature Conservation Bureau, Ministry of the Environment, Government of Japan, Tokyo (in Japanese).
Miyabuchi, Y., S. Sugiyama & Y. Nagaoka. 2012. Vegetation and fire history during the last 30,000 years based on phytolith and macroscopic charcoal records in the eastern and western areas of Aso Volcano, Japan. Quat. Int. 254: 28–35.
Murata, G. 1977. Phytogeographical consideration on the flora and vegetation of Japan. Acta Phytotax. Geobot. 28: 65–83 (in Japanese).
Murata, G. 1988. The distribution on the continental elements in Japan. Flora and its characteristic in Japan 17. Nihon No Seibutsu 2: 21–25 (in Japanese).
Mushiake, K. 2001. Hydrology and water resources in monsoon Asia. Proceedings of Symposium on Innovation Approaches for Hydrology and Water Resource Management. JSHWR. Japan, pp. 1–14.
Nei, M. 1987. Molecular Evolutionary Genetics. Columbia University Press, New York.
Noshiro, S. 2017. Vegetation history in Japan. *In*: Fukushima, T. (ed), Illustrated vegetation of Japan 2nd ed, pp. 12–14. Asakura-shoten, Tokyo (in Japanese).
Okamura, M., K. Matsufuji, H. Kimura, S. Tsuji & H. Baba. 1998. Paleolithic archaeology. Gakuseisha, Tokyo (in Japanese).
Otto-Bliesner, B. L., S. Marshall, J. T. Overpeck, G. H. Miller, A. Hu & CAPE Last Interglacial Project Members. 2006. Simulating Arctic climate warmth and icefield retreat in the Last Interglaciation. Science 311: 1751–1753.

Peakall, R. & P. E. Smouse. 2012. GenAlEx 6.5: Genetic analysis in Excel. Population genetic software for teaching and research - an update. Bioinformatics 28: 2537–2539.

Pearce, J. & S. Ferrier. 2000. Evaluating the predictive performance of habitat models developed using logistic regression. Ecol. Model. 133: 225–245.

Phillips, S. J., R. P. Anderson, M. Dudík, R. E. Schapire & M. E. Blair. 2017. Opening the black box: An open-source release of Maxent. Ecography 40: 887–893.

Powers, D. M. W. 2011. Evaluation: from precision, recall and F-measure to ROC, informedness, markedness and correlation. J. Mach. Learn. Technol. 2: 37–63.

Pritchard J. K., M. Stephens, P. Donnelly. 2000. Inference of population structure using multilocus genotype data. Genetics 155: 945–959.

Sata, H., M. Shimizu, T. Iwasaki, H. Ikeda, A. Soejima, A. E. Kozhevnikov, Z. V. Kozhevnikova, H.-T. Im, S.-K. Jang, T. Azuma, A. J. Nagano & N. Fujii. 2021. Phylogeography of the East Asian grassland plant, *Viola orientalis* (Violaceae), inferred from plastid and nuclear restriction site-associated DNA sequencing data. J. Plant Res. 134: 1181–1198.

Sakaba, T., A. Soejima, S. Fujii, H. Ikeda, T. Iwasaki, H. Saito, Y. Suyama, A. Matsuo, A. E. Kozhevnikov, Z. V. Kozhevnikova, H.-F. Wang, S.-Q, Wang, J.-H. Pak & N. Fujii. 2023. Phylogeography of the temperate grassland plant *Tephroseris kirilowii* (Asteraceae) inferred from multiplexed inter-simple sequence repeat genotyping by sequencing (MIG-seq) data. J. Plant Res. 136: 437–452.

Sramkó, G., L. Laczkó, P. A. Volkova, R. M. Bateman & J. Mlinarec. 2019. Evolutionary history of the Pasqueflowers (*Pulsatilla*, Ranunculaceae): Molecular phylogenetics, systematics and rDNA evolution. Mol. Phylogen. Evol. 135: 45–61.

Stamatakis, A. 2014. RAxML version 8: a tool for phylogenetic analysis and post-analysis of large phylogenies. Bioinformatics 30: 1312–1313.

Suyama, Y & Y. Matsuki. 2015. MIG-seq: an effective PCR-based method for genome-wide single-nucleotide polymorphism genotyping using the next-generation sequencing platform. Sci. Rep. 5: 16963.

Swets, J. A. 1988. Measuring the accuracy of diagnostic system. Science 240: 1285–1293.

Tabata, H. 1997. Meadow plants in Satoyama. *In*: Tabata, H. (ed), Satoyama and its conservation, pp 38–41. Hoikusha, Osaka (in Japanese).

Taberlet P., E. Coissac, F. Pompanon, L. Gielly, C. Miquel, A. Valentini, T. Vermat, G. Corthier, C. Brochmann, & E. Willerslev. 2007. Power and limitations of the chloroplast *trnL* (UAA) intron for plant DNA barcoding. Nucleic Acids Research 35: e14.

Takaishi, A., A. E. Kozhevnikov, Z. V. Kozhevnikova, H. Ikeda, N. Fujii & A. Soejima. 2019. Phylogeography of *Pulsatilla cernua* (Ranunculaceae), a grassland species, in Japan. Ecol. Evo. 9: 7262–7272.

Ushimaru, A., K. Uchida & T. Suka. 2018. Grassland biodiversity in Japan: threats, management and conservation. *In*: Squires, V. R., J. Dengler, H. Feng & L. Hua (eds.), Grasslands of the world, pp. 197–218. CRC Press, Boca Raton.

Varela, S., R. P. Anderson, R. Garcia-Valdes & F. Fernandez-Gonzales. 2014. Environmental filters reduce the effects of sampling bias and improve predictions of ecological niche models. Ecography 37: 1084–1091.

Watanabe, S., T. Hajima, K. Sudo, T. Nagashima, T. Takemura, H. Okajima, T. Nozawa, H. Kawase, M. Abe, T. Yokohata, T. Ise, H. Sato, E. Kato, K. Takata, S. Emori & M. Kawamiya. 2011. MIROC-ESM 2010: Model description and basic results of CMIP5-20c3m experiments. Geosci. Model Dev. 4: 845–872.

Wolfe, K. H., W.-H. Li & P. M. Sharp. 1987. Rates of nucleotide substitution vary greatly among plant mitochondrial, chloroplast, and nuclear DNAs. Proc. Natl. Acad. Sci. USA 84: 9054–9058.

Yamaura, Y., A. Narita, Y. Kusumoto, A. J. Nagano, A. Tezuka, T. Okamoto, H. Takahara, F. Nakamura, Y. Isagi & D. Lindenmayer. 2019. Genomic reconstruction of 100,000-year grassland history in a forested country: population dynamics of specialist forbs. Biol. Letters 15: 20180577.

Yurtsev, B. A. & P. G. Zhukova. 1982. Chromosome numbers of some plants of the northeastern Yakutia (the drainage of the Indigirka River in its middle reaches). Bot. Zhurn. 67: 778–787 (in Russian).

Zhang, Z. X. 2006. Karyotype analysis and cytological observation of mitosis in pasqueflora. Bull. Bot. Res., Harbin 26: 421–423.

Received June 11, 2024; accepted August 7, 2025; published February 28, 2026